Title

Stable electrospray signal on a microfabricated glass chip with three-dimensional open edge and tiered depth geometries

Authors

Schmidt, Alexander J

Zamuruyev, Konstantin O

LeVasseur, Michael K

et al.

Publication Date

2023-05-01

DOI

10.1016/j.mee.2023.111997

Peer reviewed

HHS Public Access

Author manuscript

Microelectron Eng. Author manuscript; available in PMC 2024 September 19.

Published in final edited form as:

Microelectron Eng. 2023 May 01; 276: . doi:10.1016/j.mee.2023.111997.

Stable electrospray signal on a microfabricated glass chip with three-dimensional open edge and tiered depth geometries

Alexander J. Schmidt[1,2,†], **Konstantin O. Zamuruyev**[1,2,†,‡], **Michael K. LeVasseur**[1,2,§], **Stephanie Fung**[1,2], **Ilya M. Anishchenko**[1,2,#], **Nicholas J. Kenyon**[2,3,4], **Cristina E. Davis**[1,2,3,*]

[1]Department of Mechanical and Aerospace Engineering, UC Davis, Davis, CA 95616, USA.

[2]UC Davis Lung Center, Davis CA, USA

[3]VA Northern California Health Care System, Mather CA, USA

[4]Department of Internal Medicine, UC Davis, Sacramento CA, USA

Abstract

This paper presents the microfabrication and performance of a three-dimensional electrospray ionization (ESI) emitter tip made from glass, which achieves stable current signals important for chemical analysis. Our novel microfabrication process and custom-built signal conditioning hardware provides the advantage of providing accurate features and steady signals. The fabrication process relies on standard microfabrication techniques (i.e., deposition, photolithography, and wet etching). This fabrication method involves the novel application of two layers of positive and negative photoresists in addition to Parafilm® wax tape. Open edge and tiered depth details were successfully created from a multilayer planar mask. This is a benefit for integrated miniaturized and microfluidic systems that often require micro features for their functionality but relatively large millimeter size features for their physical periphery. We demonstrate the fundamental performance of electrospray with this microfluidic chip. The emitter tip was fixed on a linear axis stage with high resolution (10 μm) to finely control the tip distance from a metal counter electrode plate. A custom printed circuit board system was built to safely control four voltages applied to the microchip ports from a single high voltage power supply. To readily form the electrospray, non-aqueous solvents were used for their low viscosity and a constant voltage of +2.7 kV was applied to the sheath electrospray microchannel. The liquid being sprayed was 80/20 (v/v) methanol/acetonitrile with 0.1% acetic acid in the sheath microchannel and with ammonium acetate (10–40 mM) in its remaining microchannels. The electrospray signal was measured in response to varying the distance (1.4 to 1.6 mm) between the electrospray emitter tip and a metal

*Correspondence: cedavis@ucdavis.edu.
‡Present address: Bionano Genomics, 6777 Nancy Ridge Drive, San Diego, CA, 92121, USA.
§Present address: Photon Ink, LLC, 11270 Sanders Dr Ste E, Rancho Cordova, CA 95742, USA
#Present address: General Atomics Aeronautical Systems, Inc., 14250 Kirkham Way, Poway, CA 92064, USA
†These authors contributed equally to this work.

Conflicts of Interest

The authors declare no competing financial interest. The electrical schematics and LabVIEW© code for data acquisition from the system is available on GitHub for non-commercial use. Please refer to Professor Cristina Davis' webpage for more information.

counter electrode plate in addition to the varying concentration of the background electrolyte, ammonium acetate. Stable and repeatable electrospray signal showed linear relationships with emitter tip distance and concentration ($r^2 \geq 0.95$).

Graphical Abstract

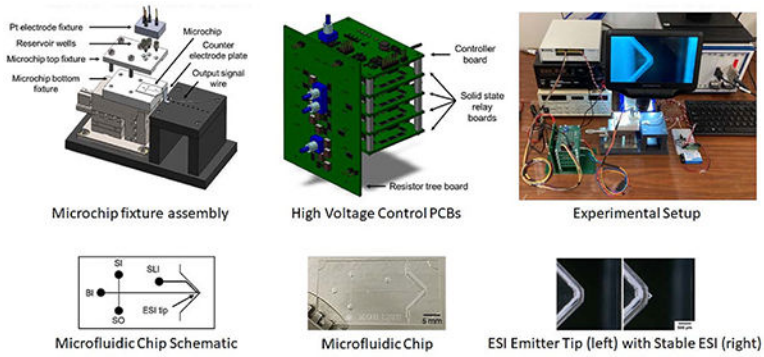

Keywords

electrospray ionization; electrospray stability; microfluidics; miniaturization; glass microfabrication; glass etching

1. Introduction

Electrospray Ionization (ESI) is a prevalent technique for liquid chemical detection in analytical chemistry.[1] ESI generates a fine liquid aerosol through electrostatic charging. A high electric potential (typically ± 2–5 kV) is applied between the end of a capillary and a counter electrode installed in proximity (typically 1–2 mm). Tiny micro–droplets tear away from the surface of a liquid Taylor cone searching for a surface to land. Due to liquid solvent evaporation and charge preservation, an emitted droplet undergoes a series of Coulomb explosions to reduce its electric repulsion between charges and achieves a charge limit corresponding to that of an ion.[2] In this way, ions contained in a liquid phase sample are transferred into a gas phase. These ions land on a counter electrode plate which can then be detected amperometrically. ESI operations are best performed in the stable cone jet mode when ESI current is most reproducible. The ability to achieve stable and effective spray depends on the applied voltage, the distance between the spray tip to the counter electrode, and the viscosity.[3] Electrospray is stable when a cone can be observed with a steady stream of droplets issued from it and when there is steady current in the external electrical circuit.

This paper presents the microfabrication and performance of a novel three-dimensional electrospray ionization (ESI) emitter tip made from glass. Only recently have three approaches been proposed for the fabrication of monolithically integrated ESI microfluidic chips from glass.[4–6] Hoffmann et al. integrated a manually pulled ESI tip onto a commercial microchip. Another approach, by Mellors et al., created an ESI tip by sawing a corner at the end of a microchannel with a dicing saw. Sainiemi et al. present parallel microfabrication of three-dimensional ESI glass emitters that are also monolithically

integrated with microfluidic channels. This approach can replace commercial electrospray needles by providing equally robust emitter tip performance. Further studies have since implemented these three techniques.[7–14] From one of these studies, a commercial chip system was developed by a startup company, 908 Devices.[12] In addition to the work presented by Sainiemi et al., our fabrication process only relies on standard microfabrication techniques (i.e., deposition, photolithography, and wet etching). We address the needs of integration of an electrospray emitter tip by considering the combination of meso- and micro-features, open edged features, and the possibility of microfabrication on a wafer scale. Our fabrication method involves the novel application of two layers of positive and negative photoresists in addition to Parafilm® wax tape. We also use isotropic wet etching of glass in hydrofluoric acid (HF) solution and chromium (Cr) deposition. This approach provides the advantage of creating a three-dimensional ESI tip with accurate and high quality small-scaled geometric features. This allows for higher charge densities leading to increased ionization efficiency for better signal stability and repeatability. Open edge and tiered depth details were successfully created from a multilayer planar mask. This is a benefit for integrated microfluidic systems that often require micro features for their functionality but large millimeter size features for their physical periphery. Dimensional control during isotropic etching is susceptible to undercutting although the etching process is beneficial when fabricating three-dimensional structures. As glass under the emitter tip is removed, a sharpened curved profile is formed with a 20 μm inner diameter.

Glass is an important material of choice for analytical and medical field applications due to its excellent material and chemical properties (i.e., mechanical strength, chemical inertness, optical transparency, and native hydrophilicity). ESI tips can be easily realized with well-established silicon microfabrication protocols, although silicon is electrically conductive and thus prevents its integration with chemical separation methods (e.g., chromatography or capillary electrophoresis) which require high voltages for operation. Polymer microfabrication also offers monolithic integration of ESI tips (SU-8 photolithography[15,16], PMMA[17], PDMS[18], polyimide[19], and thiol-ene.[20,21] However, polymers can suffer from swelling or degradation by organic solvents.[22,23]

We demonstrate the fundamental performance of electrospray with our glass microfluidic chip. This device allows efficient ionization without the use of external pressure sources. The emitter tip was fixed on a linear axis stage with high resolution (10 μm) to finely control the tip’s distance from a metal counter electrode plate. This simplified engineering testing platform allows for a more accessible electrospray stability testing procedure without the use of a mass spectrometer, a resource intensive instrument. There is limited information available in the literature that provides data on electrospray stability with this approach.[24,25] Future work for this setup envisions integration with novel micro-scaled chemical sensors to allow separation and detection of ionized molecules (e.g., high asymmetric longitudinal field ion mobility spectrometry).[26,27] This setup also has a printed circuit board system that was custom built to safely control four voltages applied to the microchip’s four ports from a single high voltage power supply. To readily form the electrospray, non-aqueous solvents were used for their low viscosity and a constant voltage of +2.7 kV was applied to the sheath electrospray microchannel. The liquid being sprayed was 80/20 (v/v) methanol/acetonitrile with 0.1% acetic acid in the sheath microchannel and with ammonium acetate

(10–40 mM) in its remaining straight cross microchannels. The electrospray signal was measured in response to varying the distance (1.4 to 1.6 mm) between the electrospray emitter tip and a metal counter electrode plate in addition to the varying concentration of the background electrolyte, ammonium acetate. Stable and repeatable electrospray signal showed linear relationships with emitter tip distance and concentration ($r^2 \geq 0.95$). Our work uniquely provides a combination of high-quality geometric features created by a novel microfabrication method, a steady electrical circuit generated by signal conditioning hardware, use of non-aqueous solutions, and fine control of emitter tip distance to a counter electrode plate. These aspects of our work allow for stable and repeatable electrospray signals.

2. Chemicals and Reagents

Acetic acid, ammonium acetate, and methanol were purchased from Sigma-Aldrich (Steinheim, Germany). Acetonitrile was purchased from Fisher Scientific (Pittsburg, PA). All chemicals and reagents were of analytical or HPLC grade. Water was purified with a Elga Purelab Classic DI Water System (Woodridge, IL). Before use, all sample and buffer solutions were filtered (0.22 μm) and degassed by sonication for 5 min.

3. Materials and Methods

The microfluidic glass chip has a monolithically integrated three-dimensional ESI emitter tip. A schematic and a photograph of the microfluidic chip are presented (Figures 1a, b). The overall length and width of the microfluidic chip are 34 and 18 mm, respectively. The buffer microchannel (buffer inlet to ESI tip) has a length of 25 mm, a depth of 100 μm, and a width of 20 μm. The sample loading microchannel (sample inlet to sample outlet) has a length of 10 mm, a depth of 100 μm, and a width of 20 μm. The sheath liquid inlet microchannel has a length of 10.8 mm, a depth of 100 μm, and a width of 200 μm. Microchannel lengths were designed to maintain electric fields (~300–500 V/cm) that are compatible with electrospray and electroosmotic flow. The chosen microchannel widths and depths are typical for microfluidic devices.[6,10] Microchannel dimensions were selected to control fluid flow, ensure sufficient chemical analysis, and controlling electric field strength. Increased microchannel widths and depths allow for higher flow rates and thus faster sample processing. However, if these dimensions increase too much, the size of droplets generated during electrospray tend to increase, which leads to reduced ionization efficiency. The sheath liquid microchannel offers the possibility to apply a voltage for ESI and functions as a buffer zone, which means the buffer inlet microchannel is not affected by the nebulized flow. The access ports have a diameter of 1.5 mm, one of which is shown in a scanning electron microscope (SEM, FEI Scios DualBeam) image (Figure 1c). These access ports are fabricated by wet etching and are thus drill-free. The bottom side cavities were etched to a depth of 560 μm which set the tip thickness and to form an open edge. The top side etch cavities were etched to a depth of 110 μm to further define the tip edge. An SEM image of the ESI emitter tip is shown (Figure 1d) as well as a side view of the ESI emitter tip (Figure 1e).

The microfluidic chip was fabricated in a class-100 cleanroom facility (Center for Nano and Micro Manufacturing, UC Davis, CA). Standard microfabrication procedures (i.e., photolithography, wet etching, and deposition) were used with Borofloat® glass, purchased from S.I. Howard Glass Co., Inc. (Worchester, MA, USA). In summary, the microchip consists of two halves: access ports and microchannels; both halves contain a part of the ESI tip. The top side of a wafer is defined to be the side that looks up when holding by the orientation of physical placement of the microchip. The bottom side of the wafer is defined to be its opposite side. The prepared glass halves were etched in 49% HF acid from both sides sequentially in order to create three-dimensional features. The chips were cleaned, and the two halves were bonded in thermal fusion. The wafers were then diced into individual chips after thermal fusion bonding. The manufacturer recommended and standard recipes were followed for microfabrication. A summarized illustration of the microfabrication process is presented (Figure 2). The access port wafer fabrication process follows a similar procedure to the microchannel wafer (described in the text below) and for simplification, is not illustrated in Figure 2.

The microfabrication process started with two clean wafers that were sputtered with 200 nm of chromium each on both sides (CHA Industries AutoTech II, Fremont, CA). The following steps apply to the access port wafer's top side and the microchannel wafer's bottom side. Images of the wafers during the fabrication process are provided (Supplemental Figure 1). Adhesion promoter hexamethyldisilazane (HMDS, Avantor Performance Materials, Inc., Center Valley, PA) was spin-coated and then with SPR 220–7.0 photoresist (Dow Electronic Materials MEGAPOSIT, Malborough, MA) to have a thickness of approximately 10 μm. The following steps apply to the access port wafer's bottom side and the microchannel wafer's top side. S1813 photoresist (Shipley, Malborough, MA) was spin-coated to have a thickness of approximately 2 μm. The access port wafer's top side and the microchannel wafer's bottom side were exposed to ultraviolet (UV) light at 250 mJ/cm^2 in hard contact mode (Karl Suss, MA4, Garching, Germany). The access port wafer's bottom side and the microchannel wafer top side were exposed to UV light at 150 mJ/cm^2 in hard contact mode. Both wafers were then developed in Microposit MF CD-26 aqueous developer (Dow Electronic Materials, Malborough, MA). The wafers were then hard baked in a vacuum oven at 155 °C for 90 min. Afterwards, both wafers were placed into a chromium etch bath (Transene Chromium Etchant 1020, Danvers, MA) for 1 min. Parafilm® tape (Bemis, Sheboygan Falls, WI) was manually applied to the access port wafer's bottom side and the microchannel wafer's top side. With separate wafers, etching rates and resulting cavity depths were determined with profilometry measurements (Dektak XT 2D, Bruker, Germany) and are shown (Supplemental Figure 2). Then, both wafers were wet etched in 49% hydrofluoric (HF) acid. The access port wafer was etched for 90 min with a etch depth of 560 μm and the microchannel wafer was etched for 85 min with an etch depth of 530 μm. Both wafers were placed in a Piranha bath to remove all photoresist.

The following steps were then applied to the microchannel wafer's top side. HMDS was spin-coated and then with SU8 3010 photoresist to have a thickness of approximately 12 μm. The wafer was exposed to UV at 130 mJ/cm^2 in hard contact mode. The wafer was then developed in SU8 developer (MicroChem Corp., Westborough, MA). SPR 220–7.0 was spin-coated to have a thickness of approximately 10 μm. The photoresist was exposed to

UV at 250 mJ/cm^2 for 2 cycles, 30 seconds apart in hard contact mode. The wafer was then developed in CD-26 aqueous developer. The wafer was then hard baked in a vacuum oven at 120 °C for 90 min. The wafer was placed in a chromium etch bath for 1 min. Parafilm® tape was manually applied on the bottom side of the wafer. The wafer was then wet etched in 49% HF acid for 17 min for an etch depth of 110 μm. The Parafilm® tape was then carefully removed. The SPR 220–7.0 layer was removed with an O_2 reactive ion etch (RIE) plasma cleaning (Plasma Equipment Technical Services, Brentwood, CA). Parafilm® tape was manually applied again on the bottom side of the wafer. The wafer was wet etched in 49% HF acid for 15 min to have an etch depth of 100 μm. The Parafilm® tape was then carefully removed. The remaining photoresist was stripped off with a Piranha bath.

The following steps were then applied to the access port wafer's bottom side. HMDS was spin-coated and then with SPR 220–7.0 to have a thickness of approximately 10 μm. The photoresist was exposed to UV at 250 mJ/cm^2 for 2 cycles, 30 seconds apart in hard contact mode. The wafer was then developed in CD-26 aqueous developer. The wafer was then hard baked in a vacuum oven at 155 °C for 90 min. Parafilm® tape was manually applied on the top side of the wafer. The wafer was placed in a chromium etch bath for 1 min. The wafer was then wet etched in 49% HF acid for 27 min for an etch depth of 175 μm. The Parafilm® tape was then carefully removed. Remaining photoresist was stripped off with a Piranha bath.

The following steps were then applied to both wafers. The wafers were placed in a chromium etch bath for 1 min. Both wafers were then placed in a Piranha bath. Both cleaned wafer halves were loaded into a plasma activation system (EVG 810, EVGroup, Austria) and the substrates were exposed to two separate capacitive coupled plasmas in sequence for a temporary bond, with a process previously described.[28] The two wafers were aligned onto each other with a mask aligner (EVG 620, EVGroup, Austria) to form the temporary bond. The wafers were then permanently bonded together using thermal fusion (EVG 501, EVGroup, Austria) for 9 hours with 19 kN pressure at 450 °C. To dice the bonded wafers into individual microfluidic chips, the wafers were loaded into a dicing saw (Disco DAD 321, Japan) with the fluid ports downwards and Kapton® tape over the ESI tips to prevent water entrance into the channels. The emitter tip was then exposed by manually snapping off the excess glass, which was made feasible with the wet etch pattern.

4. Experimental

An expanded CAD model of the microfluidic chip fixture assembly is shown (Figure 3a). The microfluidic chip is housed in a custom machined white Delrin top and bottom fixtures that are attached to PEEK™ reservoir wells (P/N: C360–405R, LabSmith, Livermore, CA) which contain the electrospray solutions. The electrode fixture contains platinum wires (23 gauge, LabSmith, Livermore, CA) that are located within the microchannel reservoir wells. The electrode fixture was 3D-printed with an Ender-3 Pro 3D Printer (Creality 3D Technology Co. Ltd, China) with polylactic acid (PLA) material. The microchip fixture subassembly was fixed onto a linear stage (ULTRAlign™ 561D-XYZ, Newport, USA) to precisely control the distance between the emitter tip and an aluminum counter electrode plate. The linear stage was mounted on top of a grey Delrin base plate. The counter electrode

plate was also mounted onto a grey Delrin base and was set at a height to be adjacent to the microchip's emitter tip. The electrospray signal from the counter electrode plate was digitized by a data acquisition system, later described. The distance between the ESI emitter tip and the counter electrode plate was determined by calibrating the known movement of the emitter tip on the linear stage with the distance travelled as displayed on the digital microscope.

The custom voltage control and signal conditioning electronics are packaged on a printed circuit board (PCB) miniaturized system. The high voltage control electronics (Figure 3b) were designed for safe use and supply of four high voltage outputs from a single high voltage power supply. High voltage supplied to the system is fed into a series of resistors which provide three intermediate voltage values. These intermediate voltages can be adjusted with potentiometers mounted on the resistor tree board. Each of the outputs to the reservoirs are controlled by custom solid-state relays, which act as single pole triple throw (SP3T) switches. Each solid-state relay board corresponds to an output for each reservoir on the microfluidic chip. On the solid-state relay board that corresponds to the electrospray reservoir, the excess current from the buffer inlet microchannel (typically ~20 μA) was grounded through a 50 MΩ coupled in parallel with the electrospray voltage supply.[6] The controller board is connected to a custom LabVIEW© software program. The relays were constructed from high voltage transistors and photovoltaic optocouplers to allow high voltage operation. Solid state relays have advantages over mechanical relays such as high reliability, long lifespan, small form factor, low power consumption, no moving parts, and silent operation. The controller board includes several LEDs to indicate the state of the outputs, including one to warn of a live high voltage supply. The controller also features analog timing circuits to ensure that no high-voltage shoot-through can occur in the relays under any switching scenario. The spacing of the components on the PCBs in the subassembly was done per the guidelines for high voltage PCB design in IPC 2221B.

The PCBs for the high voltage control system were designed using KiCad 5.1.10 open-source software (http://kicad-pcb.org/). PCBs were manufactured by BasicPCB (Aurora, CO). The PCB circuits (Supplemental Figure 3) and parts list (Supplemental Table 1) are provided in the Supplemental Information. The manufacturer recommendations were followed for assembly. The controller board and the solid-state relay boards have dimensions of 2 × 3 in., and the resistor tree board has dimensions of 3 × 4 in. These PCBs were made with FR4 material and thickness of 0.62 in. Solder paste stencils were designed and purchased from Stencils Unlimited (Lake Oswego, OR) to solder on electrical surface mount components. Electrical surface mount components were placed onto the PCBs with solder paste under a digital microscope by using tweezers and a manual pick-and-place system (SMT Caddy, CA). Once components were placed on the PCB, re-flowing the solder was carried out with an automatic reflow oven (T-962 A, Shenzhen Bangqi Chuangyuan Technology Co., Ltd., Shenzhen, China). The boards were then mounted together with nylon hardware on a 3D-printed support structure made from green PLA.

A photograph of the benchtop experimental setup is shown (Figure 3c). A high-voltage power supply (Model PS350, Stanford Research Systems, Sunnyvale, CA) was used to supply a voltage to the high voltage control electronics which then provided four voltages

to the microchannel reservoir wells. A digital microscope (Andonstar AD407, Shenzhen Andonstar Tech Co., Ltd., China) was used to display a top-down view of the electrospray at the glass emitter tip. The data acquisition was developed on National Instruments PXI hardware comprised of: PXI-1031 Chassis, Module PXI-6281, and SCB-68 I/O connector block. The electrospray current signal is conditioned with a LMC662 (Texas Instruments, Dallas, TX) in a transimpedance (current-to-voltage) amplifier configuration. The circuit was designed using a common operational amplifier integrated circuit (IC) that was powered by a single 9 V battery. Electrical schematics for the power supply of the signal conditioning system are provided (Supplemental Figure 4) and the electrical schematic for the signal conditioning circuit is provided (Supplemental Figure 5). Data were recorded at 1000 samples/s using a National Instruments I/O card and a custom LabVIEW© software program (code provided via GitHub for non-commercial use, see details below).

5. Results and Discussion

In this study, electrospray was conducted using non-aqueous solutions in positive ionization mode. Aqueous content typically has higher surface tension and thus a higher voltage is required to access the cone jet mode. Unfortunately, higher voltages with aqueous solutions increases the risk of electrochemical discharge. A mixture of methanol and acetonitrile as used in this study are commonly applied solvents and ammonium acetate is a preferred choice as a background electrolyte.[6,7,15] Non-aqueous media may be suitable for electrochemical measurements and enable detection of compounds that are otherwise difficult to oxidize or reduce under aqueous conditions.[29] For ESI, the formation of the electrospray favors lower surface tension and heat of vaporization of organic solvents.

Voltages were applied through the platinum wires placed in the microchannel reservoir wells. In the electrospray experiments, a supply voltage of +3.0 kV was provided to the high voltage control electronics. For all experiments, a voltage of +2.9 kV was supplied to the buffer inlet (BI), +2.6 kV was applied to the sample inlet (SI) and sample outlet (SO), and +2.7 kV was applied to the sheath liquid inlet (SLI). These output voltages were measured and verified with an oscilloscope (MDO3012, Tektronix, Beaverton, OR). Figure 4a shows a digital microscope image with a top-down view of the glass microfluidic chip emitter tip and Figure 4b shows a digital microscope image with a top-down view of the electrospray Taylor cone generated at the glass emitter tip. Once the voltage was applied, no accumulation of droplets at the opening tip or liquid spreading occurred. The liquid being sprayed was 80/20 (v/v) methanol/acetonitrile with 0.1% acetic acid from the SLI reservoir and 80/20 (v/v) methanol/acetonitrile with ammonium acetate at a concentration of 20 mM from the remaining three reservoirs. The electrical conductivity of this solution was measured to be 1335 μS/cm with an Orion Star™ A212 Conductivity Benchtop Meter (Fisher Scientific, Pittsburg, PA). While observing the ESI signal intensity, the linear stage adjusted the position of the integrated emitter tip with respect to the counter electrode plate, and then the spray voltage initiated.

Figure 5 shows the signal response of electrospray to the distance between the emitter tip and the counter electrode plate. Distances from the emitter tip to the counter electrode plate from 1600 to 1400 μm with 50 μm intervals and 1 min durations. A current pulse is

observed in the first interval which can be attributed to the electrical current induced by a voltage change. The PEEK™ reservoir wells have a volume of 85 μL, which is sufficient to providing solution for electrospray for at least 5 min. The signal demonstrates that the integrated emitter tip is efficient at generating a stable electrospray at varying emitter tip distances. The emitter tip geometry is sufficiently sharp to facilitate the formation of a Taylor cone immediately when the ESI voltage is applied and adjusting the emitter tip distance. These data are similar to the results presented by Kang et al.[25] In this work, an experimental setup for automatic control of single capillary electrospray was developed. A syringe pump was used to inject a spray solution into a stainless-steel capillary (ID 90 μm, OD 224 μm), which was approximately 5 mm from an orifice plate. The liquids being sprayed included 80/20 (v/v) isopropanol/water and ammonium acetate with electrical conductivities 782 and 346 μS/cm. Electrospray currents were approximately 150–225 nA with a voltage range 950–1250 V.

Replicated signal response data of electrospray ionization to the distance between the electrospray emitter tip and the metal counter electrode plate are shown (Figure 6a). The liquid being sprayed was 80/20 (v/v) methanol/acetonitrile with 0.1% acetic acid from the SLI reservoir and 80/20 (v/v) methanol/acetonitrile with ammonium acetate (20 mM) from the remaining three reservoirs. Data are averaged over 1 min durations for n=5 replicates. The ESI signal ranged from approximately 80 to 200 nA. These data obtained for the distance sweep resulted a correlation coefficient of r^2=0.99. Figure 6b shows replicate signal response data of electrospray ionization to the concentration of ammonium acetate at an emitter distance of 1600 μm. The liquid being sprayed was the same as was done in Figure 6a with varying concentrations of ammonium acetate. Data are averaged over 1 min durations for n=5 replicates. The ESI signal ranged from approximately 50 to 150 nA. These data obtained in the concentration sweep resulted a correlation coefficient r^2=0.95.

From the results shown, the system provides good electrospray stability and reproducibility. The emitter tip geometry is sufficiently sharp to avoid potential liquid-spreading and to decrease the required voltage for establishing a stable Taylor cone. High-resolution control of the emitter tip distance from the counter electrode plate by using a high-resolution linear stage allows for precise measurements of electrospray signal dependency on distance. The solvents used in this study, methanol, and acetonitrile, have lower viscosities compared to water. This lower viscosity allows for a lower electrospray onset voltage thus avoiding electrical discharge. Ammonium acetate is used as a typical BGE at low concentrations (10–40 mM) due to its high volatility and compatibility with established separation and analysis methods (i.e., capillary electrophoresis, mass spectrometry). Reproducible and stable data were shown for the dependence of the electrospray signal on the concentration of ammonium acetate. Live video feedback from a digital microscope used to display the electrospray emitter tip and formation of the Taylor cone was particularly useful to determine the experimental parameters (onset voltage and emitter tip distance) necessary for functional ESI. Fine control of emitter tip distance was achieved with the use of a linear stage with 10 μm resolution. This allows for highly precise adjustments to achieve conditions appropriate for electrospray. Additionally, our novel microfabrication method, custom-built signal conditioning hardware, and use of non-aqueous solutions provide a system that can perform stable and repeatable electrospray ionization signal.

6. Conclusion

In this work, we present the microfabrication and operation of a three-dimensional electrospray ionization (ESI) emitter tip made from glass. Our fabrication process relies on standard microfabrication techniques, yet it involves the novel application of two layers of positive and negative photoresists in addition to Parafilm® wax tape. Open edge and tiered depth details were successfully created from a multilayer planar mask. We demonstrate the fundamental performance of electrospray with this microfluidic chip. The emitter tip was fixed on a linear axis stage with high resolution to finely control the tip's distance from a metal counter electrode plate. High voltage control electronics were developed to safely supply four voltages applied to the microchip's four ports from a single high voltage power supply. To readily form the electrospray, non-aqueous solvents were used for their low viscosity and a constant voltage of +2.7 kV was applied to the sheath electrospray microchannel. The liquid being sprayed was 80/20 (v/v) methanol/acetonitrile with 0.1% acetic acid in the sheath microchannel and with ammonium acetate (10–40 mM) in its remaining microchannels. The electrospray signal was measured in response to varying the distance (1.4 to 1.6 mm) between the electrospray emitter tip and a metal counter electrode plate in addition to the varying concentration of the background electrolyte, ammonium acetate. Stable and repeatable electrospray signal showed linear relationships with emitter tip distance and concentration ($r^2 \geq 0.95$). Data were also shown for the dependence of the electrospray signal on the concentration of ammonium acetate. Live video feedback from a digital microscope used to display the electrospray emitter tip and formation of the Taylor cone was particularly useful to determine the experimental parameters (onset voltage and emitter tip distance) necessary for functional ESI. This work contributes towards the development of a system that may surpass limitations presented by mass spectrometry. High cost and large instrumentation associated with mass spectrometry are setbacks that may be avoided with a micro-scaled system. Stable electrospray from a microfluidic device will be a critical component for the interface between future developed microsystems that include liquid separation and the detection of ionized molecules. Further work envisions the development and testing of the experimental design and setup with microfluidic chemical separation methods (e.g., capillary electrophoresis) and its integration with novel micro-scaled chemical sensors to allow further separation and detection of ionized molecules (e.g., high asymmetric longitudinal field ion mobility spectrometry).[26,27] Further work also envisions the use of the electronics for precise voltage switching times between sample injection and separation modes. These novel concepts may be applied to medical analyses and clinical diagnostics for enhanced portability, reliability, and throughput.[30]

Supplementary Material

Refer to Web version on PubMed Central for supplementary material.

Acknowledgements

Partial support was provided by NIH awards: U01 EB0220003-01 (CED, NJK); UL1 TR001860 (CED, NJK); 1P30ES023513-01A1 (CED, NJK); UG3-OD023365 (CED, NJK); 1U18TR003795-01 (CED, NJK), 4U18TR003795-02 (CED, NJK); and 1U01TR004083-01 (CED, NJK). Partial support was also provided by: the Department of Veterans Affairs award I01 BX004965-01A1 (CED, NJK); the University of California Tobacco-Related Disease Research Program award T31IR1614 (CED, NJK); and University of California CITRIS and the

Banatao Institute award 19-0092 (CED, NJK). Trainee support was provided by NIH TL1 TR001861 (AJS) and T32 HL07013 (KOZ). The contents of this manuscript are solely the responsibility of the authors and do not necessarily represent the official views of the funding agencies. The authors gratefully acknowledge access and use of the UC Davis Center for Nano and Micro Manufacturing (CNM2). The authors also gratefully acknowledge Mitchell McCartney, Patrick Gibson, Bradley Chew, and Jean-Pierre Delplanque (University of California, Davis) for technical discussions.

Acronyms:

BI	buffer inlet
CAD	computer aided design
Cr	chromium
DI water	deionized water
ID	inner diameter
LED	light emitting diode
PCB	printed circuit board
PDMS	polydimethylsiloxane
Piranha	mixture of H_2SO_4:H_2O_2 at 4:1 ratio
OD	outer diameter
PLA	polylactic acid
PMMA	polymethylmethacrylate
Pt	platinum
sccm	standard cubic centimeters per minute
SEM	scanning electron microscope
SI	sample inlet
SLI	sheath liquid inlet
SO	sample outlet
SP3T	single pole triple throw

References

1. Prudent M and Girault HH. (2009) Functional electrospray emitters. Analyst 134: 2189–2203. DOI:10.1039/b910917j. [PubMed: 19838404]
2. Wilm M (2011) Principles of Electrospray Ionization. Molecular & Cellular Proteomics 10: M111.009407. DOI:10.1074/mcp.m111.009407.
3. Cech NB and Enke CG. (2001) Practical implications of some recent studies in electrospray ionization fundamentals. Mass Spectrometry Reviews 20: 362–387. DOI:10.1002/mas.10008. [PubMed: 11997944]

4. Hoffmann P, Häusig U, Schulze P and Belder D (2007) Microfluidic glass chips with an integrated nanospray emitter for coupling to a mass spectrometer. Angewandte Chemie - International Edition 46: 4913–4916. DOI:10.1002/anie.200605152. [PubMed: 17516595]
5. Mellors JS, Gorbounov V, Ramsey RS and Ramsey JM. (2008) Fully integrated glass microfluidic device for performing high-efficiency capillary electrophoresis and electrospray ionization mass spectrometry. Analytical Chemistry 80: 6881–6887. DOI:10.1021/ac800428w. [PubMed: 18698800]
6. Sainiemi L, Sikanen T and Kostiainen R (2012) Integration of fully microfabricated, three-dimensionally sharp electrospray ionization tips with microfluidic glass chips. Analytical Chemistry 84: 8973–8979. DOI:10.1021/ac301602b. [PubMed: 23045954]
7. Fritzsche S, Hoffmann P and Belder D (2010) Chip electrophoresis with mass spectrometric detection in record speed. Lab on a Chip 10: 1227–1230. DOI:10.1039/c000349b. [PubMed: 20445873]
8. Mellors JS, Jorabchi K, Smith LM and Ramsey JM. (2010) Integrated microfluidic device for automated single cell analysis using electrophoretic separation and electrospray ionization mass spectrometry. Analytical Chemistry 82: 967–973. DOI:10.1021/ac902218y. [PubMed: 20058879]
9. Fritzsche S, Ohla S, Glaser P, Giera DS, Sickert M, Schneider C and Belder D (2011) Asymmetric organocatalysis and analysis on a single microfluidic nanospray chip. Angewandte Chemie - International Edition 50: 9467–9470. DOI:10.1002/anie.201102331. [PubMed: 21948447]
10. Chambers AG, Mellors JS, Henley WH and Ramsey JM. (2011) Monolithic integration of two-dimensional liquid chromatography-capillary electrophoresis and electrospray ionization on a microfluidic device. Analytical Chemistry 83: 842–849. DOI:10.1021/ac102437z. [PubMed: 21214194]
11. Chambers AG and Ramsey JM. (2012) Microfluidic dual emitter electrospray ionization source for accurate mass measurements. Analytical Chemistry 84: 1446–1451. DOI:10.1021/ac202603s. [PubMed: 22220742]
12. Batz NG, Mellors JS, Alarie JP and Ramsey JM. (2014) Chemical vapor deposition of aminopropyl silanes in microfluidic channels for highly efficient microchip capillary electrophoresis-electrospray ionization-mass spectrometry. Analytical Chemistry 86: 3493–3500. DOI:10.1021/ac404106u. [PubMed: 24655020]
13. Black WA, Stocks BB, Mellors JS, Engen JR and Ramsey JM. (2015) Utilizing Microchip Capillary Electrophoresis Electrospray Ionization for Hydrogen Exchange Mass Spectrometry. Analytical Chemistry 87: 6286–6287. DOI:10.1021/acs.analchem.5b01179.
14. Redman EA, Batz NG, Mellors JS and Ramsey JM. (2015) Integrated microfluidic capillary electrophoresis-electrospray ionization devices with online ms detection for the separation and characterization of intact monoclonal antibody variants. Analytical Chemistry 87: 2264–2272. DOI:10.1021/ac503964j. [PubMed: 25569459]
15. Sikanen T, Tuomikoski S, Ketola RA, Kostiainen R, Franssila S and Kotiaho T (2007) Fully microfabricated and integrated SU-8-based capillary electrophoresis-electrospray ionization microchips for mass spectrometry. Analytical Chemistry 79: 9135–9144. DOI:10.1021/ac071531+. [PubMed: 17973354]
16. Nordman N, Sikanen T, Aura S, Tuomikoski S, Vuorensola K, Kotiaho T, Franssila S and Kostiainen R (2010) Feasibility of SU-8-based capillary electrophoresis-electrospray ionization mass spectrometry microfluidic chips for the analysis of human cell lysates. Electrophoresis 31: 3745–3753. DOI:10.1002/elps.201000373. [PubMed: 21077242]
17. Li FA, Huang JL and Her GR. (2008) Chip-CE/MS using a flat low-sheath-flow interface. Electrophoresis 29: 4938–4943. DOI:10.1002/elps.200800271. [PubMed: 19130573]
18. Sikanen T, Aura S, Franssila S, Kotiaho T and Kostiainen R (2012) Microchip capillary electrophoresis-electrospray ionization-mass spectrometry of intact proteins using uncoated Ormocomp microchips. Analytica Chimica Acta 711: 69–76. DOI:10.1016/j.aca.2011.10.059. [PubMed: 22152798]
19. Yin H, Killeen K, Brennen R, Sobek D, Werlich M and Van De Goor T (2005) Microfluidic chip for peptide analysis with an integrated HPLC column, sample enrichment column, and nanoelectrospray tip. Analytical Chemistry 77: 527–533. DOI:10.1021/ac049068d. [PubMed: 15649049]

20. Tähkä SM, Bonabi A, Jokinen VP and Sikanen TM. (2017) Aqueous and non-aqueous microchip electrophoresis with on-chip electrospray ionization mass spectrometry on replica-molded thiol-ene microfluidic devices. Journal of Chromatography A 1496: 150–156. DOI:10.1016/j.chroma.2017.03.018. [PubMed: 28347516]
21. Lu N, Petersen NJ, Kretschmann AC and Kutter JP. (2021) Non-aqueous electrophoresis integrated with electrospray ionization mass spectrometry on a thiol-ene polymer–based microchip device. Analytical and Bioanalytical Chemistry DOI:10.1007/s00216-021-03374-9.
22. Sun X, Kelly RT, Tang K and Smith RD. (2010) Ultrasensitive nanoelectrospray ionization-mass spectrometry using poly(dimethylsiloxane) microchips with monolithically integrated emitters. The Analyst 135: 2296. DOI:10.1039/c0an00253d. [PubMed: 20617264]
23. Geczy R, Sticker D, Bovet N, Häfeli UO and Kutter JP. (2019) Chloroform compatible, thiol-ene based replica molded micro chemical devices as an alternative to glass microfluidic chips. Lab on a Chip 19: 798–806. DOI:10.1039/c8lc01260a. [PubMed: 30688958]
24. Si Y, Yang Y, Martel M, Zhang L, Kirychuk S, Predicala B and Guo H (2021) Characterization of electrical current and liquid droplets deposition area in a capillary electrospray. Results in Engineering 9: 100206. DOI:10.1016/j.rineng.2021.100206.
25. Kang S, Chen AB, Yu T, Yang Y, Gui H, Liu J and Chen DR. (2022) A new spray current control for the reliable operation of a single-capillary electrospray. Journal of Aerosol Science 166: 106073. DOI:10.1016/j.jaerosci.2022.106073.
26. Zrodnikov Y, Rajapakse MY, Peirano DJ, Aksenov AA, Kenyon NJ and Davis CE. (2019) High Asymmetric Longitudinal Field Ion Mobility Spectrometry Device for Low Power Mobile Chemical Separation and Detection. Analytical Chemistry 91: 5523–5529. DOI:10.1021/acs.analchem.8b05577. [PubMed: 30932473]
27. Fung S, Levasseur MK, Rajapakse MY, Chew BS, Fung AG, Mccartney MM, Kenyon NJ and Davis E (2022) Sensors and Actuators : A . Physical Battery powered dual-polarity ion detector for trace chemical sensing. Sensors and Actuators: A. Physical 338: 113442. DOI:10.1016/j.sna.2022.113442.
28. Boden S, Karam P, Schmidt A and Pennathur S (2017) A process to fabricate fused silica nanofluidic devices with embedded electrodes using an optimized room temperature bonding technique. Applied Physics Letters 110: DOI:10.1063/1.4982968.
29. Cassidy J, Khoo SB, Pons S and Fleischmann M (1985) Electrochemistry at very high potentials: The use of ultramicroelectrodes in the anodic oxidation of short-chain alkanes. Journal of Physical Chemistry 89: 3933–3935. DOI:10.1021/j100264a034.
30. Davis CE, Frank M, Mizaikoff B and Oser H (2010) Editorial The Future of Sensors and Instrumentation for Human Breath Analysis. IEEE Sensors Journal 10: 3–6. DOI:10.1109/JSEN.2009.2035675.

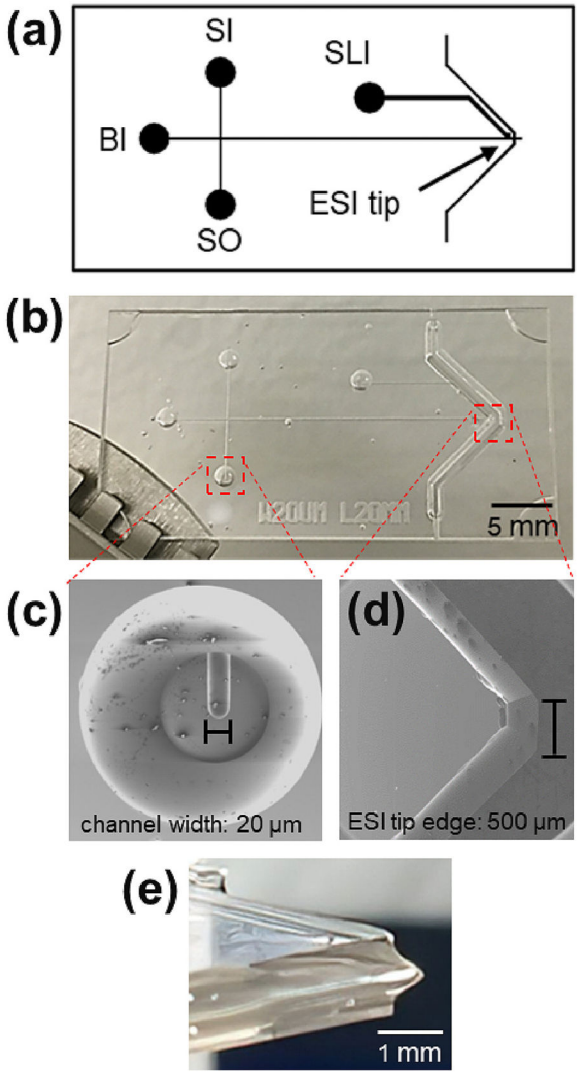

Figure 1.

(a) Schematic of the microfluidic chip layout. SI: sample inlet, SO: sample outlet, BI: buffer inlet, SLI: sheath liquid inlet. All microchannels have a depth of 100 μm. The buffer microchannel (BI to ESI tip) has a length of 25 mm and a width of 20 μm. The sample loading microchannel (SI to SO) has a length of 10 mm and a width of 20 μm. The SLI microchannel has a length of 10.8 mm and a width of 200 μm. **(b)** Photograph of the microfluidic chip with an integrated electrospray emitter tip, held by a tweezer after dicing. **(c)** Scanning electron microscope (SEM) image of drill-free reservoir port. **(d)** Top-down view SEM image of the ESI emitter tip. **(e)** Side view photo of the ESI emitter tip.

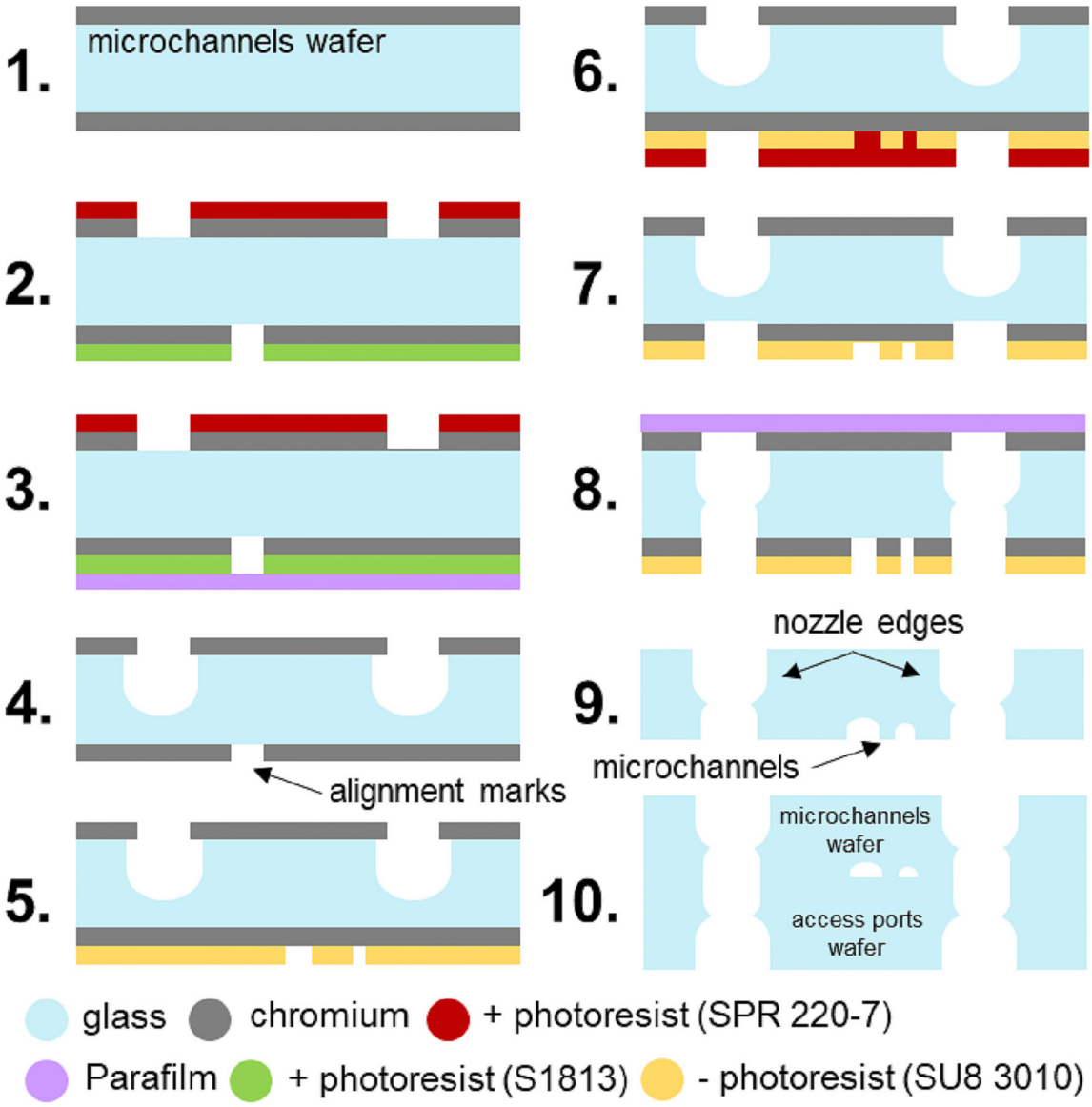

Figure 2.

Summary and illustration of the microfabrication process. The microfabrication process for the access ports wafer is excluded due to redundancy. **1.** Start with new glass wafer and sputter chromium (Cr) both sides. **2.** Apply SPR 220–7 on top side, S1813 on bottom side. UV exposure to define ESI tip edge on top side. UV exposure to define alignment marks on bottom side. Develop both sides. Etch Cr both sides. **3.** Apply Parafilm® tape on bottom side. **4.** Etch glass in HF and remove both photoresists and Parafilm® tape. Alignment marks remain on bottom side. **5.** Apply SU8 3010 on bottom side. UV exposure to define microchannels on bottom side (alignment marks not illustrated for simplification). Develop SU8 3010 on bottom side. **6.** Apply SPR 220–7 on bottom side. UV exposure to define ESI tip and alignment marks (not shown) on bottom side. Develop SPR 220–7. **7.** Etch Cr and etch glass in HF. Remove SPR 220–7. **8.** Etch Cr and etch glass in HF with Parafilm® applied on bottom side. **9.** Remove SU8 3010 and Parafilm®. Etch Cr both sides.

10. Surface plasma activation and thermal fusion bonding of the access ports wafer and the microchannels wafer.

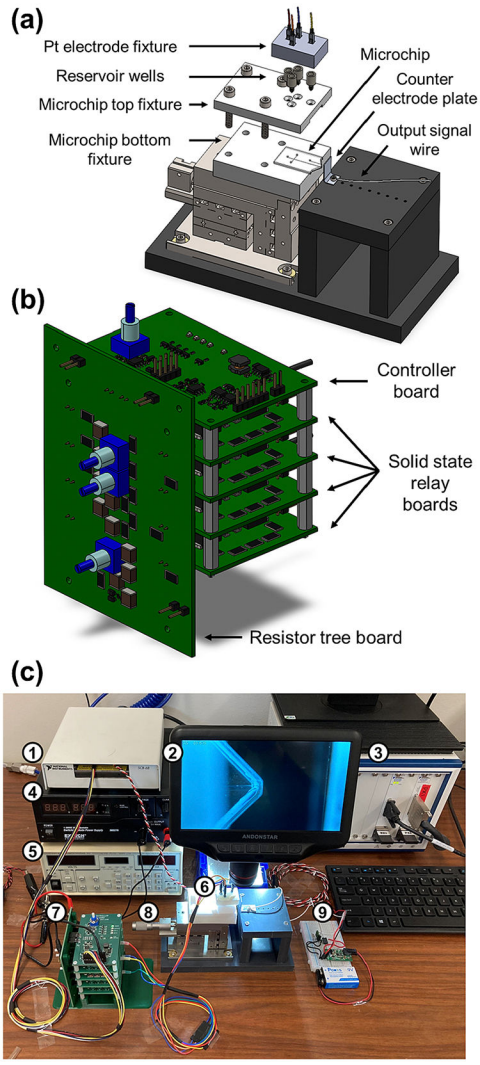

Figure 3.

(a) Expanded microchip fixture assembly consisting of the linear stage, the microchip and its top and bottom fixtures, the Pt electrode fixture, and counter electrode plate. **(b)** Electronics for the control of four voltages from a single high voltage source. **(c)** Photograph of the experimental setup. **1.** National Instruments connector block. **2.** Digital microscope displaying a top-down view of the glass emitter tip. **3.** National Instruments Chassis. **4.** DC power supply for a vacuum pump (not shown). **5.** High voltage power supply. **6.** Microchip fixture and Pt electrode fixture. **7.** High voltage control electronics. **8.** Linear stage. **9.** Signal conditioning electronics.

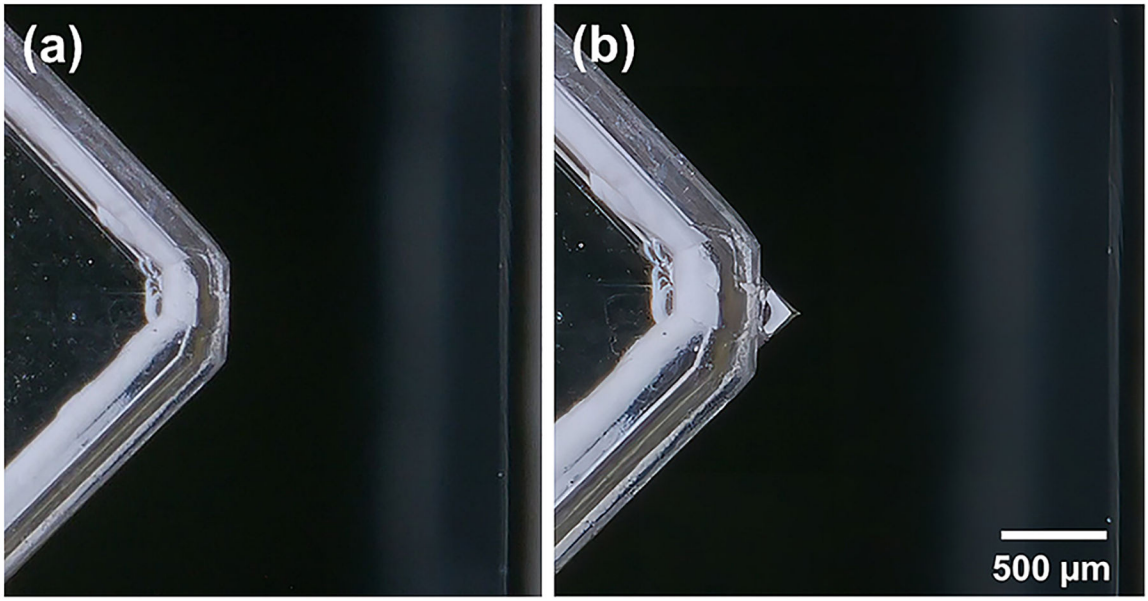

Figure 4.

(a) Digital microscope image with a top-down view of the glass microfluidic chip emitter tip. **(b)** Digital microscope image with a top-down view of the electrospray Taylor cone generated at the glass emitter tip. The liquid being sprayed was 80/20 (v/v) methanol/acetonitrile with 0.1% acetic acid from the Sheath Liquid Interface (SLI) reservoir and 80/20 (v/v) methanol/acetonitrile with ammonium acetate at a concentration of 20 mM from the remaining three reservoirs.

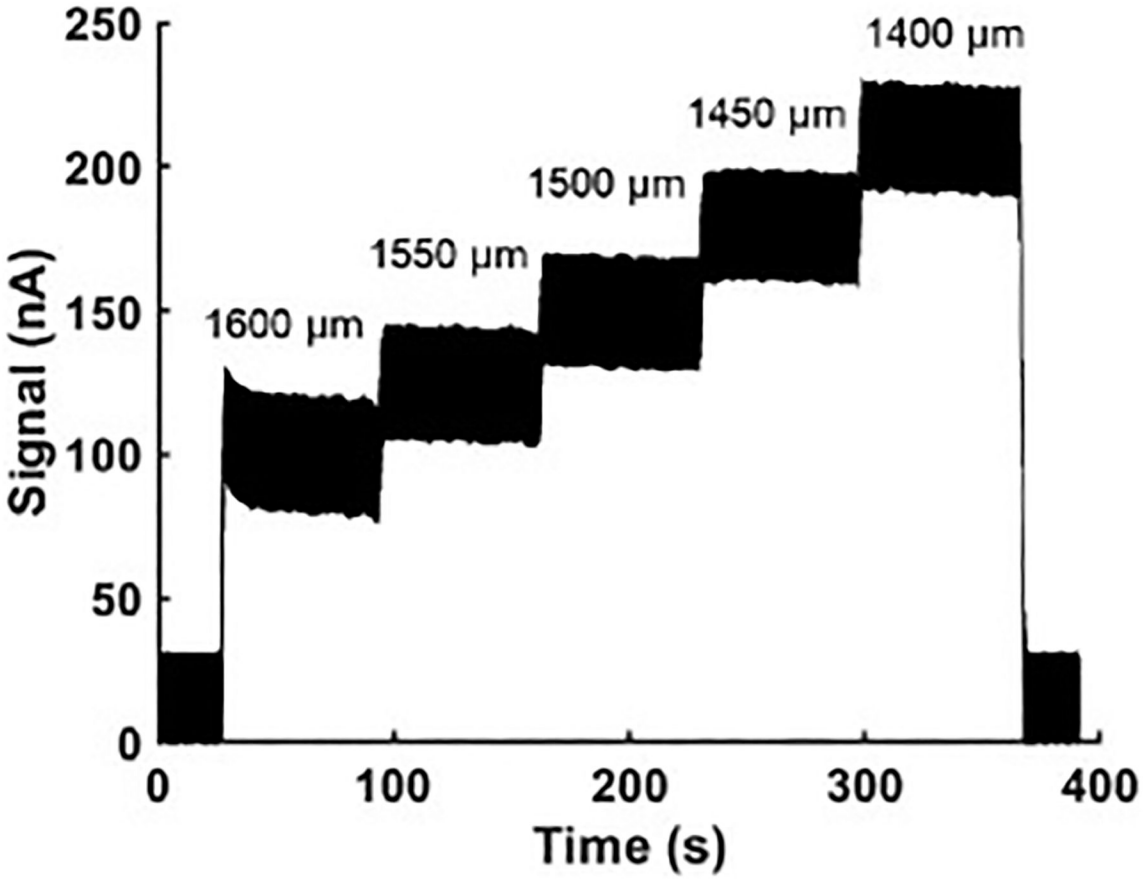

Figure 5.

Signal response of electrospray ionization to the distance between the electrospray emitter tip and the metal counter electrode plate. The liquid being sprayed was 80/20 (v/v) methanol/acetonitrile with 0.1% acetic acid from the Sheath Liquid Inlet (SLI) reservoir and 80/20 (v/v) methanol/acetonitrile with ammonium acetate at a concentration of 20 mM from the remaining three reservoirs. A constant voltage of +2.7 kV was applied to the SLI reservoir to perform electrospray.

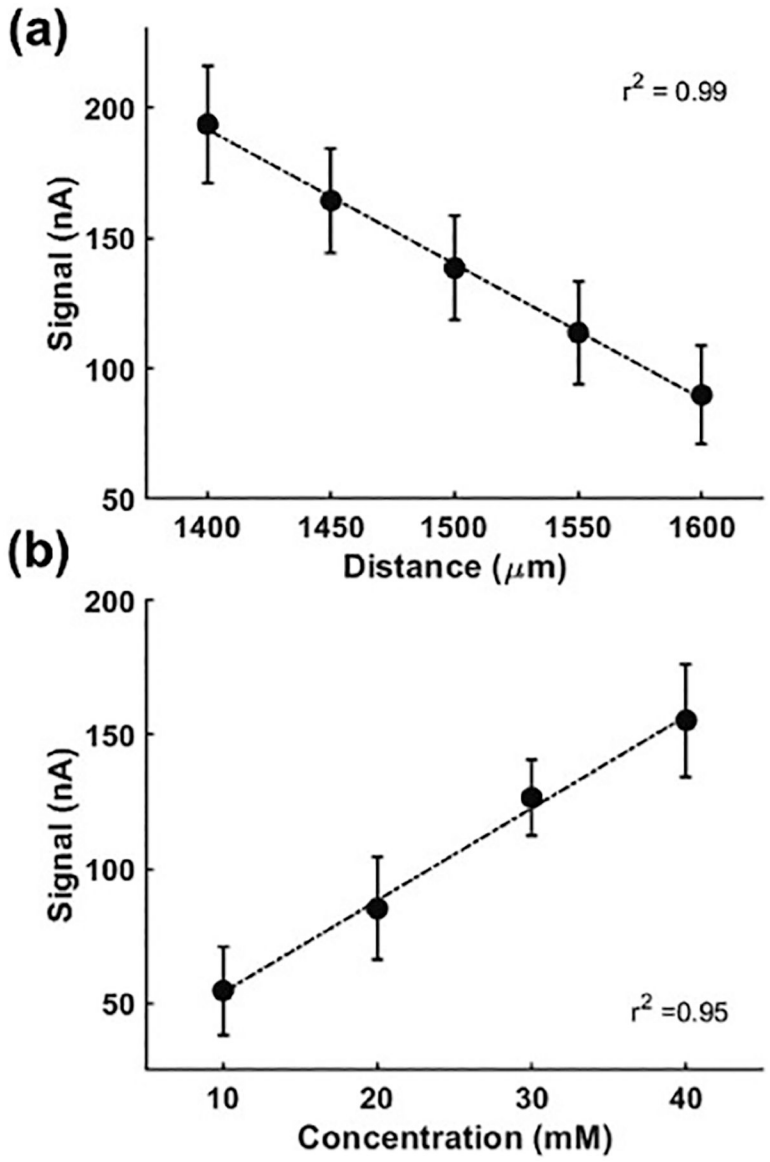

Figure 6.

(a) Signal response of electrospray ionization to the distance between the electrospray emitter tip and the metal counter electrode plate. The liquid being sprayed was 80/20 (v/v) methanol/acetonitrile with 0.1% acetic acid from the Sheath Liquid Inlet (SLI) reservoir and 80/20 (v/v) methanol/acetonitrile with ammonium acetate at a concentration of 20 mM from the remaining three reservoirs. A constant voltage of +2.7 kV was applied to the SLI reservoir to perform electrospray. Data are averaged over 1 min durations for n=5 replicates. **(b)** Signal response of electrospray ionization to the concentration of ammonium acetate at an emitter distance of 1600 μm. The liquid being sprayed, and voltage applied to the SLI reservoir were the same as was done in caption (a) with varying concentrations. Data are averaged over 1 min durations for n=5 replicates.